Received: 30 November 2015 | Revised: 22 August 2016 | Accepted: 23 August 2016

DOI 10.1111/cmi.12660

WILEY

RESEARCH ARTICLE

Type I interferon promotes cell-to-cell spread of *Listeria monocytogenes*

Suzanne E. Osborne[1†] | Brandon Sit[1,2†] | Andrew Shaker[1,3] | Elissa Currie[1,3] | Joël M.J. Tan[1] | Jorik van Rijn[1] | Darren E. Higgins[4] | John H. Brumell[1,3,5,6]

[1] Cell Biology Program, Hospital for Sick Children, Toronto, Ontario, Canada

[2] Department of Immunology, University of Toronto, Toronto, Ontario, Canada

[3] Department of Molecular Genetics, University of Toronto, Toronto, Ontario, Canada

[4] Department of Microbiology and Immunology, Harvard Medical School, Boston, Massachusetts, USA

[5] Institute of Medical Science, University of Toronto, Toronto, Ontario, Canada

[6] SickKids IBD Centre, Hospital for Sick Children, Toronto, Ontario, Canada

Correspondence
John H. Brumell, Cell Biology Program, Hospital for Sick Children, 686 Bay Street, PGCRL, Room 19.9706, Toronto, ON M5G 0A4, Canada.
Email: john.brumell@sickkids.ca

Funding information
Canadian Institutes of Health Research, MOP#136973.

Summary

Type I interferons (IFNs) play a critical role in antiviral immune responses, but can be deleterious to the host during some bacterial infections. *Listeria monocytogenes* (*Lm*) induces a type I IFN response by activating cytosolic antiviral surveillance pathways. This is beneficial to the bacteria as mice lacking the type I IFN receptor (IFNAR1$^{-/-}$) are resistant to systemic infection by *Lm*. The mechanisms by which type I IFNs promote *Lm* infection are unclear. Here, we show that IFNAR1 is required for dissemination of *Lm* within infection foci in livers of infected mice and for efficient cell-to-cell spread *in vitro* in macrophages. IFNAR1 promotes ActA polarization and actin-based motility in the cytosol of host cells. Our studies suggest type I IFNs directly impact the intracellular life cycle of *Lm* and provide new insight into the mechanisms used by bacterial pathogens to exploit the type I IFN response.

1 | INTRODUCTION

Release of type I interferons (IFNs) by mammalian cells is a critical antiviral defense mechanism (Schneider, Chevillotte, & Rice, 2014), though less is known about their role during bacterial infections. Mounting evidence indicates that for some pathogens of clinical concern, type I IFNs exacerbate infection (Auerbuch, Brockstedt, Meyer-Morse, O'Riordan, & Portnoy, 2004, Carrero, Calderon, & Unanue, 2004, O'Connell et al., 2004; Henry, Brotcke, Weiss, Thompson, & Monack, 2007, Dorhoi et al., 2014). The mechanisms by which type I IFNs promote bacterial infection remain unclear (Eshleman & Lenz, 2014, McNab, Mayer-Barber, Sher, Wack, & O'Garra, 2015).

Listeria monocytogenes (*Lm*) is a foodborne pathogen responsible for listeriosis in humans; a disease characterized by meningoencephalitis and septicaemia. *Lm* has a remarkable intracellular life cycle characterized by an ability to spread non-lytically to neighboring cells (Ireton, 2013; Kuehl, Dragoi, Talman, & Agaisse, 2015). Following invasion into host cells, *Lm* uses the pore-forming toxin listeriolysin O and two phospholipases to escape from its vacuolar environment. Taking advantage of the nutrient-rich cytosol, *Lm* rapidly replicates. Using a cell surface bound virulence protein (ActA), *Lm* recruits the host actin-nucleating complex Arp2/3, leading to the formation of actin "clouds" around the bacteria. ActA localization becomes polarized on the surface of *Lm*, leading to the formation of actin "comet tails" that drive bacterial motility in the cytosol (Lambrechts, Gevaert, Cossart, Vandekerckhove, & Van Troys, 2008). When motile *Lm* contacts the plasma membrane, they can induce the formation of actin-rich structures resembling filopodia, called protrusions. A complex interplay of host and microbial factors are required for protrusion formation, recognition, and engulfment by neighboring cells (Robbins et al., 1999; Chong, Squires, Swiss, & Agaisse, 2011, Ireton, 2013; Czuczman et al., 2014; Ireton, Rigano, Polle, & Schubert, 2014, Rigano, Dowd, Wang, & Ireton, 2014, Talman, Chong, Chia, Svitkina, & Agaisse, 2014, Fattouh et al., 2015; Gianfelice et al., 2015). Once engulfed by neighboring cells, *Lm* escapes from a double membrane compartment (called the secondary vacuole) to perpetuate infection (Grundling, Gonzalez, & Higgins, 2003).

[†] These authors contributed equally to the work.

Following entry into the host cytosol, *Lm* induces a robust expression of type 1 IFN (O'Riordan, Yi, Gonzales, Lee, & Portnoy, 2002, Hansen et al., 2014). Several groups have demonstrated that type I IFN production promotes *Lm* infection: IFNAR1$^{-/-}$ mice are more resistant to systemic *Lm* infection compared to wild-type mice (Auerbuch et al., 2004; Carrero et al., 2004; O'Connell et al., 2004). It has been suggested that resistance stems, in part, from the ability of IFNβ to sensitize lymphocytes to apoptosis (Carrero et al., 2004), to restrict neutrophil recruitment to the site of infection (Brzoza-Lewis, Hoth, & Hiltbold, 2012) and to attenuate the production of IFNγ (Rayamajhi, Humann, Penheiter, Andreasen, & Lenz, 2010). Whether type I IFNs directly impact the intracellular life cycle of *Lm* during infection has not been examined.

Here, we examined the role of type 1 IFNs in cell-to-cell spread by *Lm*, since this process is critically required for the virulence of these and other bacterial pathogens. We demonstrate that type I IFNs promote cell-to-cell spread of *Lm* both *in vitro* and *in vivo*. IFNAR1 was found to promote ActA polarization and actin-based motility. Thus, type 1 IFN signaling is required for efficient transfer of bacteria from infected cells to neighboring cells to perpetuate infection. Our study reveals a role for type I IFNs in modulating a key step in cell-to-cell spread of a bacterial pathogen, contributing to the understanding of how type I IFNs impact host-pathogen interactions.

2 | RESULTS

2.1 | IFNAR1 promotes *Lm* cell-to-cell spread during systemic infection of mice

Mice lacking the type I IFN receptor (IFNAR1$^{-/-}$) are more resistant to systemic infection by *Lm* (Auerbuch et al., 2004; Carrero et al., 2004; O'Connell et al., 2004). The mechanism for this resistance remains unclear. To address this question, we infected C57BL/6 and IFNAR1$^{-/-}$ mice with *Lm* by tail vein injection and examined bacterial burden 3 days post-infection. Consistent with prior studies, IFNAR1$^{-/-}$ mice were more resistant to systemic infection, displaying a decreased number of CFU in the spleen and liver (Figure S1). We observed increased cell density in the infection foci of C57BL/6 relative to IFNAR1$^{-/-}$ (Figure 1a) consistent with the impact of type I IFNs on the host immune response including neutrophil recruitment (Brzoza-Lewis et al., 2012).

Lm colonizes tissues at distinct infection foci where they undergo cell-to-cell spreading events (Leung, Gianfelice, Gray-Owen, & Ireton, 2013). Liver sections from IFNAR1$^{-/-}$ mice consistently displayed a significant decrease in the size of the infection focus (Figure 1a and 1b) and the number of infected cells per focus (Figure 1a and 1c). These results suggested that, *in vivo*, the ability of *Lm* to disseminate through host tissue is restricted in mice lacking IFNAR1.

2.2 | IFNAR1 promotes *Lm* cell-to-cell spread *in vitro*

To further examine the role of type 1 IFN in *Lm* cell-to-cell spread, we performed an *in vitro* infection focus assay (Alberti-Segui, Goeden, & Higgins, 2007, Czuczman et al., 2014). Confluent monolayers of bone marrow-derived macrophages (BMDMs) from control (C57BL/6) or IFNAR1$^{-/-}$ mice were infected with *Lm* at a low multiplicity of infection (MOI) for 20 hr. Infection foci were imaged using immunofluorescence microscopy to assess cell-to-cell spread (Figure 2a). IFNAR1$^{-/-}$ BMDMs had a significant decrease in both the infection focus area (Figure 2b) and the number of infected cells per focus (Figure 2c) relative to control cells.

Infection with *Lm* induces robust expression of IFNβ (O'Riordan et al., 2002; Hansen et al., 2014). Neutralization of IFNβ with a blocking antibody caused a significant decrease in cell-to-cell spread in control cells but had no effect in IFNAR1$^{-/-}$ BMDMs, indicating that the IFNAR1$^{-/-}$ defect stems from an inability to recognize IFNβ (Figure 2a–c). Addition of recombinant IFNβ to control BMDMs had little effect on *Lm* cell-to-cell spread, suggesting saturation of type 1 IFN signaling during infection. Addition of recombinant IFNβ to IFNAR1$^{-/-}$ BMDMs had no effect, as expected. Together, our results indicate that IFNAR1 promotes cell-to-cell of *Lm* both *in vitro* and *in vivo*.

We monitored cell-to-cell spread using live cell imaging between 6 and 21 hr post-infection (Figure 3a; Images of infected cells were captured every 15 min). The RFP-*Lm* voxel volume (a proxy for bacterial spread) was consistently reduced in infected IFNAR1$^{-/-}$ BMDMs relative to control (Figure 3b). This suggested that IFNAR1 may be required for a key step in the life cycle of *Lm* in host cells that impacts its ability to spread from infected cells to neighboring cells.

2.3 | IFNAR1 is not required for intracellular growth of *Lm*

Lm grows rapidly in the cytosol of host cells. We considered the possibility that IFNAR1 promotes cell-to-cell spread of *Lm* by affecting the intracellular growth of these bacteria. To test this idea, we infected C57BL/6 and IFNAR1$^{-/-}$ BMDMs with *Lm* at a low MOI and examined bacterial burden over 24 hr of infection (Figure S2a). We used Δ*actA* mutant *Lm* since these bacteria escape vacuoles and replicate normally in the cytosol (Brundage, Smith, Camilli, Theriot, & Portnoy, 1993) but do not undergo actin-based motility, thereby avoiding any confounding effects of cell-to-cell spread. There was no significant difference in intracellular growth of Δ*actA Lm* during infection of C57BL/6 and IFNAR1$^{-/-}$ BMDMs. Thus, the defect in cell-to-cell spread of *Lm* in IFNAR1$^{-/-}$ cells is not due to differences in intracellular bacterial growth rate.

2.4 | Type 1 IFN signaling promotes *Lm* cell-to-cell spread in HeLa cells

To test whether the effect of type 1 IFN was limited to macrophages, we examined cell-to-cell spread in HeLa cells. Addition of recombinant IFNβ significantly increased spread of *Lm* in HeLa cells as measured by a 4-day plaque assay (Figure S3a and S3b) without impacting intracellular replication of bacteria in the cytosol (Figure S2b). Together, these findings indicate that the effect of type 1 IFN on *Lm* cell-to-cell spread is not limited to macrophages.

2.5 | IFNAR1 promotes protrusion formation but not their association with neighboring cells

Next, we performed a cell-to-cell spread assay (Alberti-Segui et al., 2007; Czuczman et al., 2014) to further examine the role of IFNAR1

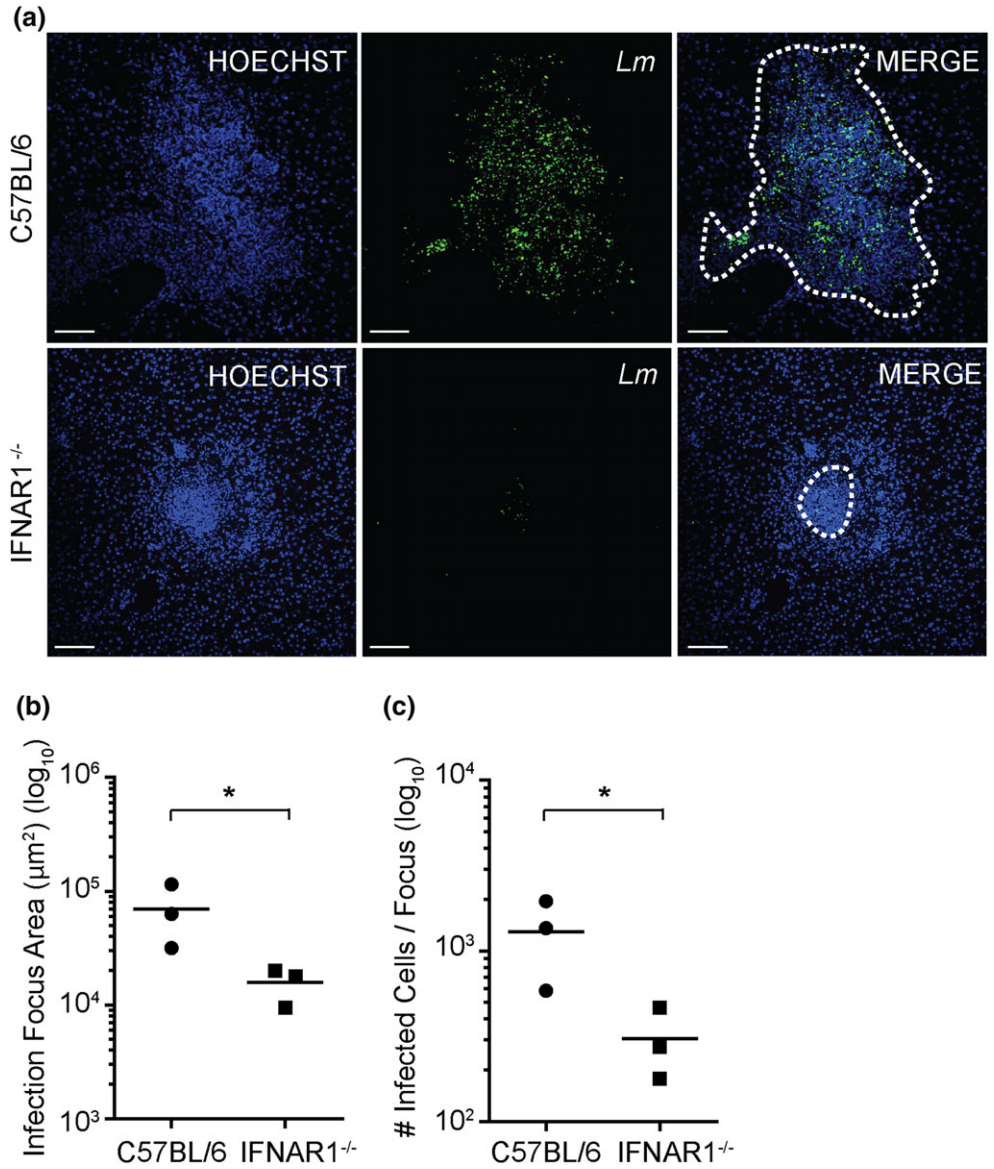

FIGURE 1 IFNAR1 promotes *Lm* cell-to-cell spread during systemic infection of mice. C57BL/6 and IFNAR1$^{-/-}$ mice were infected i.v. for 72 hr. Livers sections were stained for *Lm* and cell nuclei (Hoechst) and imaged by confocal microscopy. (a) Representative images of stained liver sections (10× magnification, scale = 70 μm). Dotted line represents the outer limits of an infection focus. These images were used to determine (b) the area of each infection focus and (c) the number of infected cells per focus (number of Hoechst nuclei within an infection focus). Each point represents a single mouse from which at least 12–30 foci were quantified per mouse. (*$p < 0.05$)

in dissemination of *Lm*. The advantage of this assay is that it enables differentiation of molecular events required in either the primary infected cell (also referred to as the "sending" cell) and neighboring secondarily infected (or "receiving") cells. BMDMs were infected for 3 hr with a Δ*plcA*Δ*plcB* mutant of *Lm*, which is unable to escape the secondary vacuole during cell-to-cell spread. Primary infected BMDMs were overlaid onto CellTracker Blue-labeled secondary cells for 90 min. Spreading events were imaged by confocal microscopy. Using this assay, we observed a significant decrease in the formation of cell-surface protrusions in IFNAR1$^{-/-}$ primary cells relative to control regardless of secondary cell genotype (Figure 4a and 4b).

We previously showed that protrusion uptake by secondary cells is enhanced by TIM-4, which can bind to exofacial phosphatidylserine (PS) present on the protrusion of the primary cell (Czuczman et al., 2014). Loss of TIM-4 affects the number of protrusions from primary infected cells associated with secondary cells (Czuczman et al., 2014). Thus, it was possible that IFNAR1 promotes protrusion association with secondary cells. However, we observed that when IFNAR1$^{-/-}$ BMDMs were the primary infected cell, there was no significant difference in the relative number of protrusions associated with secondary cells relative to control BMDMs (Figure 4a and 4c). These data indicate that IFNAR1 is required for efficient cell-to-cell spread by acting in the primary infected (sending) cell to promote protrusion formation, but not through recognition of protrusions by neighboring cells.

2.6 | IFNAR1 promotes the formation of actin comet tails

Protrusion formation by *Lm* requires actin-based motility (Monack & Theriot, 2001). Therefore, we assessed the ability of *Lm* to undergo

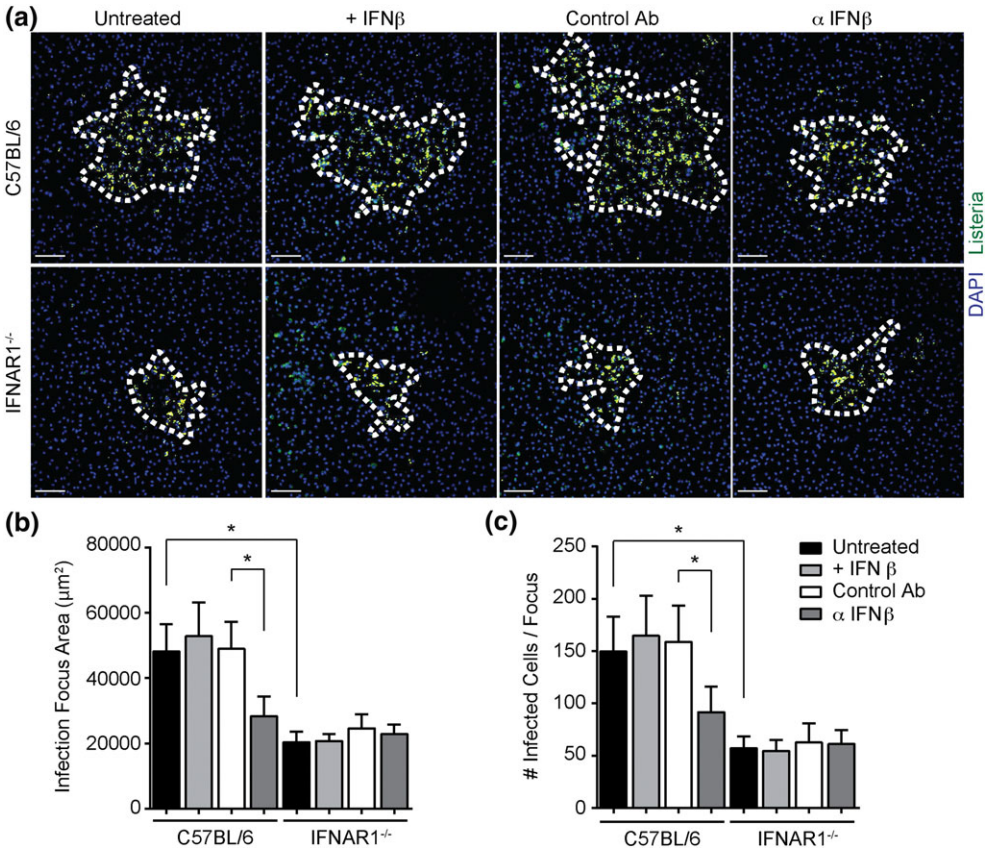

FIGURE 2 IFNAR1 promotes *Lm* cell-to-cell spread *in vitro*. Bone marrow-derived macrophages (BMDMs) were generated from C57BL/6 and IFNAR1$^{-/-}$ mice. Confluent monolayers were infected with a low MOI of *Lm* for 20 hr and analyzed by immunofluorescence microscopy. Recombinant IFNβ, an IFNβ neutralizing antibody (α IFNβ), or control antibody were added as indicated. (a) Representative images of the infection foci are shown. Dotted lines indicate the leading edge of the infection focus. Scale = 70 μm. Software was utilized to quantify (b) the focus area and (c) the number of *Lm*-associated cells per focus (identified by DAPI stained nuclei) (n = 3, N > 50 images, $^*p$ < 0.05)

actin-based motility, focusing first on the ability of these bacteria to form actin comet tails at 7-hr post-infection in C57BL/6 and IFNAR1$^{-/-}$ BMDMs using confocal microscopy. There were significantly fewer comet tails formed per bacterium in IFNAR1$^{-/-}$ cells relative to control (Figure 5a and 5b) but comet tail length and protrusion length was not affected (Figure 5c). Furthermore, more perinuclear *Lm* were observed in IFNAR1$^{-/-}$ BMDMs, indicative of reduced motility of intracellular bacteria (Figure 5a).

2.7 | IFNAR1 promotes actin-based motility by *Lm*

We further examined the role of IFNAR1 in actin-based motility using live cell imaging. BMDMs were infected with RFP-*Lm* for 4 hr, and actin dynamics were assessed using the cell permeable SiR-actin probe every 15 s for 4 min. *Lm* was equally capable of recruiting actin to form actin clouds in IFNAR1$^{-/-}$ BMDMs compared to control (Figure 6a and 6b; Supplemental Movie 3 and 4).

The Arp2/3 complex is the actin nucleator commandeered by the *Lm* virulence factor ActA for cytosolic motility (Domann et al., 1992; Kocks et al., 1992; Welch, Iwamatsu, & Mitchison, 1997). Expression of the Arp2 component of the Arp2/3 complex has been shown to be upregulated by IFNβ-treatment in fibroblasts and B cells (Pfeffer et al., 2004; Chang et al., 2007; Rusinova et al., 2013). To test whether Arp2 expression in BMDMs requires IFNAR1, lysates from C57BL/6 and IFNAR1$^{-/-}$ cells infected for 4 hr with *Lm* were probed for Arp2 by immunoblotting. Arp2 levels were not reduced in IFNAR1$^{-/-}$ BMDMs (Figure S4). These findings are consistent with equivalent formation of actin clouds around bacteria in the IFNAR1$^{-/-}$ BMDMs (Figure 6a and 6b) and suggest that the *Lm* motility defect observed in IFNAR1$^{-/-}$ is not due to Arp2/3 availability.

Of the *Lm* that successfully recruited actin, there was a significant decrease in the number of motile bacteria in IFNAR1$^{-/-}$ cells (Figure 6c). IFNAR1 did not have a significant impact on the speed of motile *Lm* (Figure 6d) nor on the total number of intracellular *Lm* (Figure 6e). These results indicate that in IFNAR1$^{-/-}$ cells, *Lm* can form actin clouds but has a reduced ability to transition to actin-based motility. However, once formed, the actin comet tails appear fully functional. We conclude that IFNAR1 impacts the intracellular lifestyle of *Lm* in a manner that promotes cell-to-cell spread by these bacteria.

2.8 | IFNAR1 promotes ActA polarization

Lm cytosolic motility requires unipolar redistribution of ActA on the bacterial surface, a process that involves both host and bacterial factors (Kocks et al., 1992; Rafelski & Theriot, 2005, Rafelski & Theriot, 2006). To examine the role of IFNAR1 in this process,

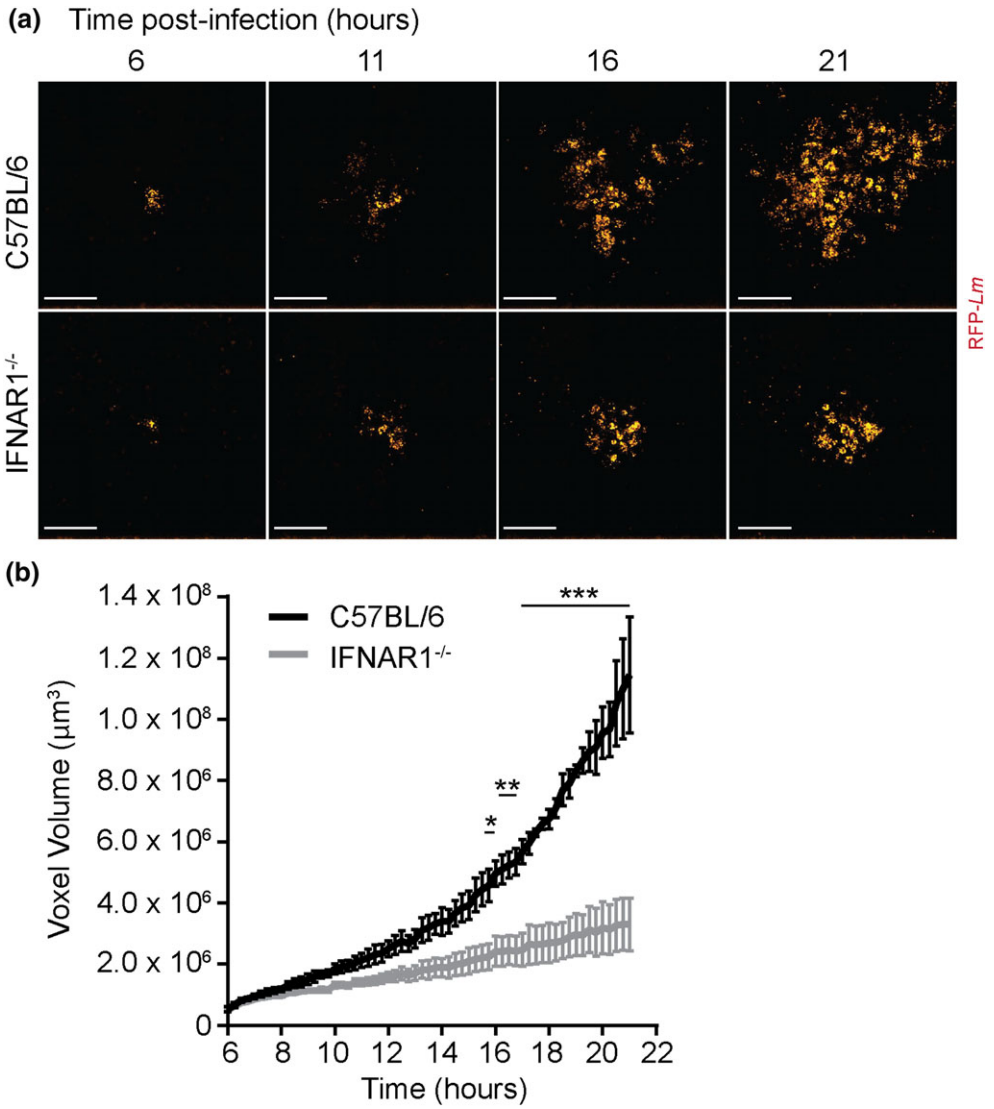

FIGURE 3 Loss of IFNAR1 leads to a consistent defect in cell-to-cell spread by *Lm*. Confluent bone marrow-derived macrophage (BMDM) monolayers from C57BL/6 and IFNAR1$^{-/-}$ mice were infected with a low MOI of RFP-expressing *Lm*. Cell-to-cell spread was examined using live cell microscopy over 21 hr. (a) Representative images captured at the indicated times during a live cell imaging experiment. Scale = 100 µm. (b) RFP voxel volume was quantified as a proxy for bacterial spread at each time point. (n = 3, N = 10, *p < 0.05, **p < 0.01, ***p < 0.001, Bonferroni's multiple comparisons test, and two-way ANOVA.)

BMDMs were infected for 4 hr and ActA localization was examined using confocal microscopy. As expected in C57BL/6 cells, approximately 70% of *Lm* displayed unipolar localization of ActA (Figure 7 a and 7b). However, in IFNAR1$^{-/-}$ BMDMs, there was a significant decrease in the number of *Lm* with unipolar ActA. There was no difference in the number of bacteria that stained positive for ActA, indicating expression of this virulence factor was not affected (Figure 7c). We reasoned that the decreased number of *Lm* with unipolar ActA in IFNAR1$^{-/-}$ could be due to a defect in bacterial cell division, a process required for ActA polarization (Kocks et al., 1992, Rafelski & Theriot, 2005, Rafelski & Theriot, 2006). However, there was no difference in the number of doublet *Lm* (*Lm* that had divided but not yet separated) in IFNAR1$^{-/-}$ BMDMs relative to control cells (Figure 7d). These results indicate that IFNAR1 promotes ActA polarization without affecting bacterial cell division.

3 | DISCUSSION

It is well established that mice lacking the type I interferon receptor IFNAR1 are resistant to systemic *Lm* infection yet the mechanism for this resistance has been unclear (Auerbuch et al., 2004; Carrero et al., 2004; O'Connell et al., 2004). Here, we provide the first evidence that IFNAR1 is required for efficient cell-to-cell spread of *Lm*, a critical step in its infection process. In contrast to prior studies pointing to alterations in the immune response to *Lm* infection (Eshleman et al., 2014, McNab et al., 2015), our studies indicate that type 1 IFN impacts directly on the intracellular lifestyle of *Lm*.

Many pathogens are known to modulate the actin cytoskeleton of host cells during infection (de Souza Santos & Orth, 2015). In our studies, we observed that actin-based motility by *Lm* is impaired in IFNAR1$^{-/-}$ BMDM. While still able to recruit actin into clouds around bacteria, the loss of IFNAR1 decreased the ability of *Lm* to initiate actin-based

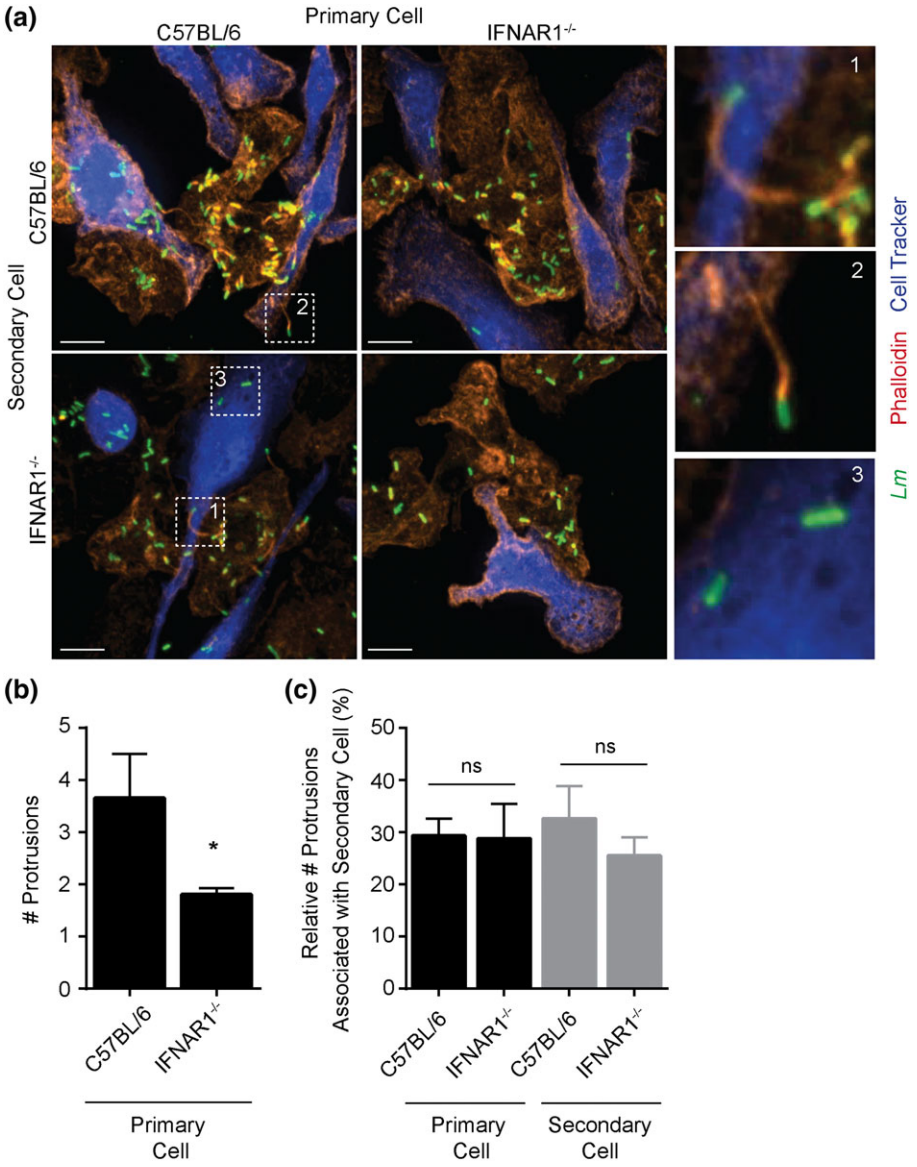

FIGURE 4 IFNAR1 promotes protrusion formation but not their association with neighboring cells. Cell-to-cell spread assay: C57BL/6 and IFNAR1$^{-/-}$ bone marrow-derived macrophages (BMDMs) were infected with Δ*plcA*Δ*plcB* mutant *Lm* for 3 hr and overlayed onto Cytotracker Blue-labeled C57BL/6 or IFNAR1$^{-/-}$ secondary cells. After 90 min, cells were fixed and stained for *Lm* and F-actin was labeled with phalloidin. (a) Representative immunofluorescence images of primary infected cells overlayed onto secondary cells (blue) in all four phenotypic combinations. Enlarged panel 1: example of a protrusion originating from a primary cell and contacting a secondary cell. Panel 2: example of a protrusion formed by primary cell but failing to contact a secondary cell. Panel 3: *Lm* successfully transferred to a secondary cell. Scale = 11 μm. Images used to quantify (b) the total number of protrusions formed by primary cells and (c) the fraction of protrusions that were associated with secondary cells. Alternating primary and secondary cell genotypes were included. (n = 3, N = 20, $^*p < 0.05$)

motility, likely through a defect in ActA polarization. A reduction in the number of motile *Lm* led to a corresponding drop in the number of protrusions formed, therefore limiting cell-to-cell spread. It is worth noting that the length of actin comet tails and protrusions, and speed were unaffected by loss of IFNAR1, suggesting that these structures underwent normal actin polymerization/depolymerization reactions once formed.

Our findings suggest that the transition from actin clouds to motile actin comet tails requires IFNAR1. This process, referred to as "motility maturation" (Rafelski & Theriot, 2005), is a poorly understood step in the intracellular life cycle of *Lm*. Initial studies suggested that bacterial cell division was sufficient for polarization of actin on the surface of *Lm*, leading to motility of bacteria (Tilney & Portnoy, 1989, Tilney, DeRosier, & Tilney, 1992). However, simultaneous live cell imaging of ActA and polymerized actin on the *Lm* cell surface revealed a high degree of heterogeneity in motility maturation, and that a variety of host and bacterial factors impact this process (Rafelski & Theriot, 2005). Motility maturation may be controlled by host regulators of actin polymerization as the host cytoskeleton was recently shown to bias the *Lm* intracellular division cycle towards bacteria forming actin comet tails (Siegrist et al., 2015). Our studies indicate that motility maturation by *Lm* requires type 1 IFN-responsive genes. The identity of these genes and the mechanisms by which they promote actin-based motility by *Lm* will be an important topic for future studies.

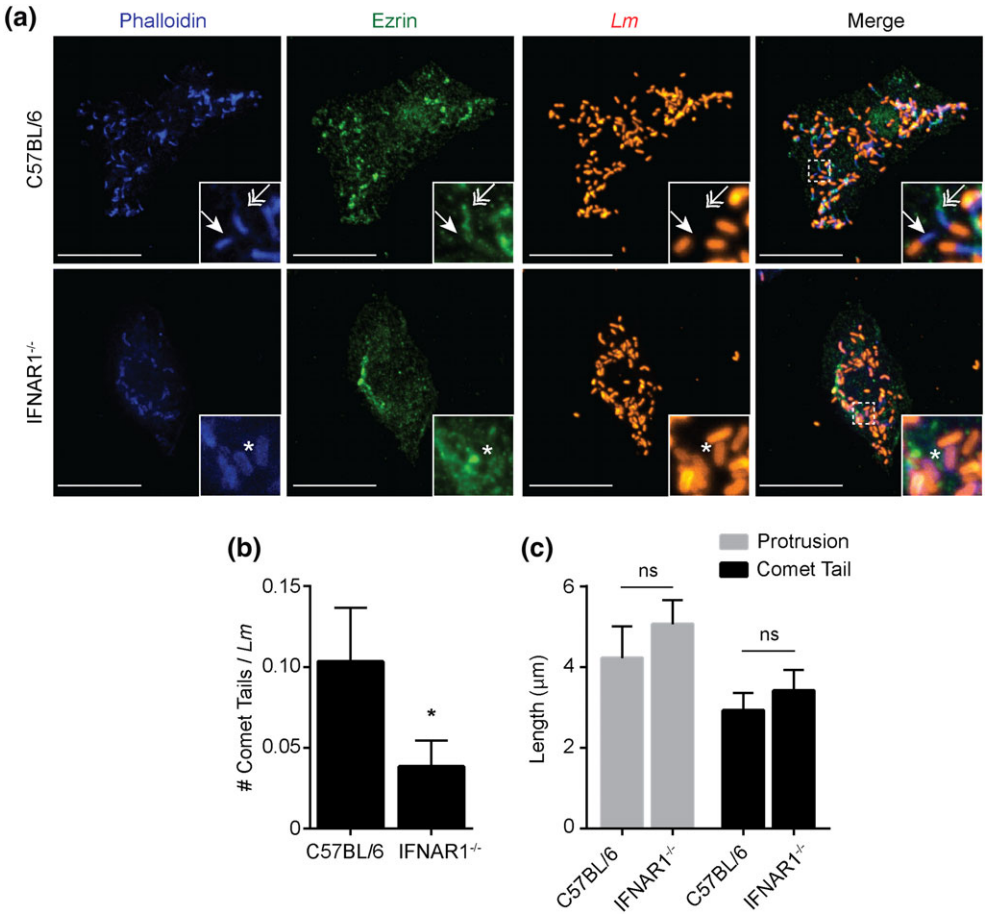

FIGURE 5 IFNAR1 promotes the formation of actin comet tails. Bone marrow-derived macrophages (BMDMs) from C57BL/6 and IFNAR1$^{-/-}$ were infected with *Lm* for 7 hr and then cells were fixed and stained for F-actin (phalloidin) and the protrusion marker ezrin. (a) Representative images. Zoomed-in panels display comet tails (single-headed arrow: phalloidin^{+} and ezrin^{-}, within the cell plane) and protrusions (double-headed arrow: phalloidin^{+} and ezrin^{+}, outside the cell plane). Scale = 11 μm. Images were used to quantify (b) the number of comet tails per *Lm* and (c) the length of protrusions and comet tails. (n = 3, N = 20 cells, $^{*}p < 0.05$)

Whether other bacterial pathogens exploit type 1 IFN to promote their actin-based motility in the cytosol (e.g., *Shigella flexneri*, *Burkholderia pseudomallei*, *Mycobacterium marinum*, and *Rickettsia ricketsiae*) will also be in important question.

Our findings highlight the importance of type 1 IFN regulation in the context of bacterial infections. Our studies also provide support for the development of novel therapies to block type 1 IFN during infection by pathogens like *Lm* that exploit this host response. The type 1 IFN response and its impact on host–pathogen interactions will continue to be an important topic for future studies.

4 | EXPERIMENTAL PROCEDURES

4.1 | Bacterial strains

All strains were on a *Listeria monocytogenes* 10403S (Bishop & Hinrichs, 1987) (wild-type) background and were generously provided by Daniel A. Portnoy, University of California at Berkeley: Δ*plcA*Δ*plcB* (DP-L1936) (Smith et al., 1995), Δ*actA* (DP-L3078) (Skoble, Portnoy, & Welch, 2000). Wild-type *Listeria monocytogenes* 10403S expressing TagRFP under the *actA* promoter (RFP-*Lm*; DP-L5538) was previously described (Waite et al., 2011). For routine propagation, bacteria were grown in brain-heart infusion broth at 30°C. For infection studies, bacteria were grown at 37°C with aeration.

4.2 | Antibodies and reagents

Recombinant IFNβ (reactive with mouse and human IFNAR1) was used at 500 U/ml (PeproTech, 300-02 BC). The following primary antibodies were used: rabbit anti-*Lm* (BD 223021; 1:200), rat anti-mouse IFNβ (PBL Interferon Source 22400–1; 1 μg/ml), rat IgG (BioLegend 400401; 1 μg/ml), mouse anti-ezrin (Invitrogen, #35–7300; 1:100), and rabbit anti-ActA (Gift from Pascale Cossart, Institut Pasteur; 1:200). Secondary antibodies including Alexa Fluor 568 Phalloidin (Life Technologies A12380), Alexa Fluor 405 Phalloidin (Biotium 00034), goat anti-rabbit 488 (Molecular Probes A11070), goat anti-rabbit 568 (Molecular Probes A11036), and goat anti-mouse 488 (Molecular Probes A11029) were used at 1:200. DAPI (Invitrogen, #D1306) was used at 1:2500 dilution. Acti-Stain 670 was used at 1:200 (Cytoskeleton, PHDN1). CellTracker Blue (Molecular Probes C2110) was used at 20 μM to stain cells. For live cell imaging, SiR-actin probe (1 μM; Cytoskeleton Inc., #CY-SC006) was added.

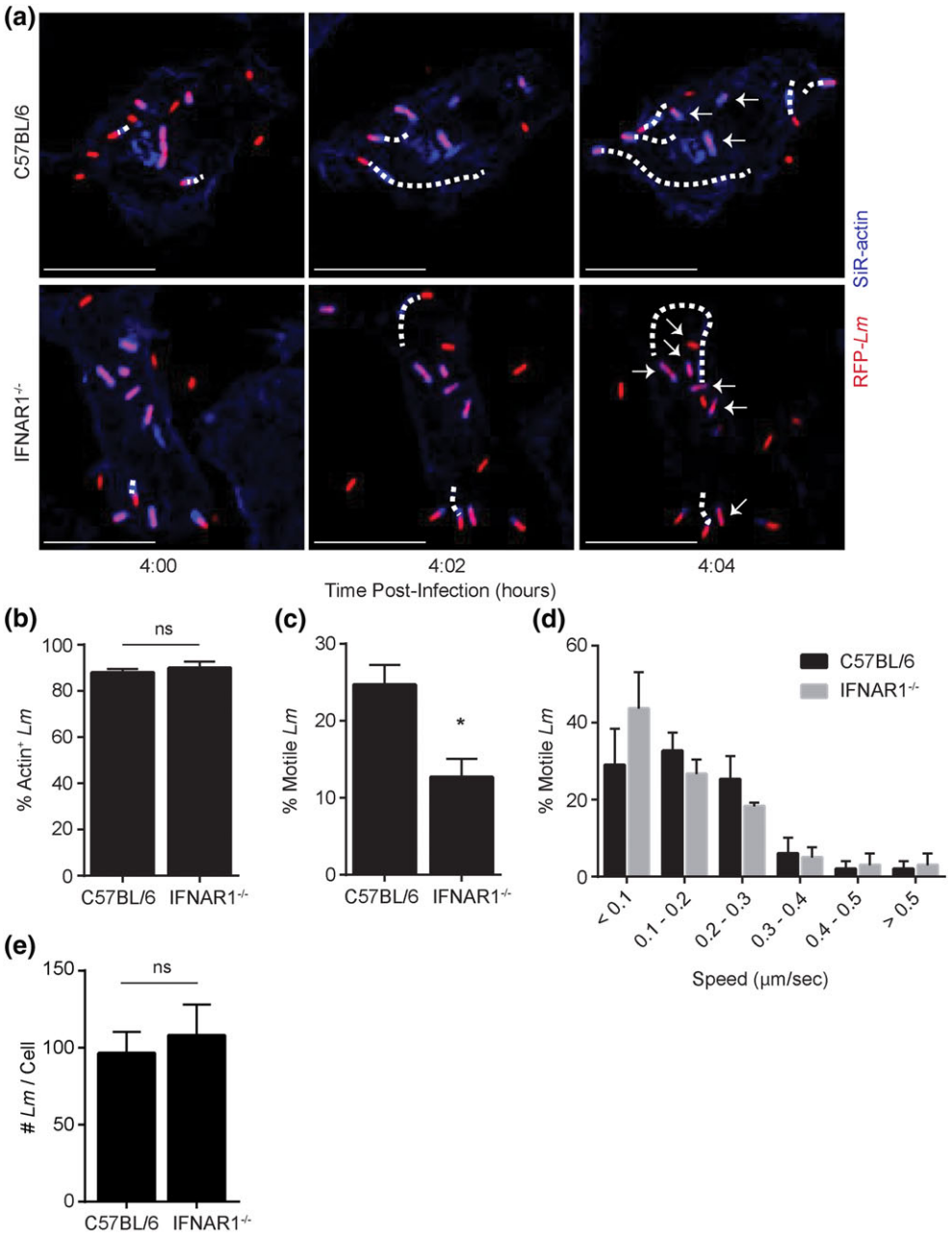

FIGURE 6 IFNAR1 promotes actin-based motility by *Lm*. C57BL/6 and IFNAR1$^{-/-}$ bone marrow-derived macrophages (BMDMs) were infected with RFP-*Lm* and actin dynamics were examined by live cell imaging at 4-hr post infection using cell-permeable SiR-actin stain. (a) Representative images from live cell imaging experiment. Dotted lines track the path of motile *Lm*. Arrows indicate *Lm* in actin clouds that did not transition to comet tails. Scale = 15 µm. Movies were used to quantify (b) the percent of *Lm* that recruited actin, (c) the percent of *Lm* that were motile, (d) the speed of bacteria, and (e) the total number of intracellular *Lm* (n = 3, N = 10 cells, $^*p < 0.05$)

4.3 | Animals

IFNAR1$^{-/-}$ mice were obtained from the Mutant Mouse Resource and Research Centers (032045-JAX) (Muller et al., 1994). C57BL/6 mice, originally from The Jackson Laboratory (Bar Harbor, ME) were used as controls. All mice were bred in house at the Hospital for Sick Children Research Institute Animal Care Facility and used in accordance with the Guide for the Humane Use and Care of Laboratory Animals. All protocols were approved by the Hospital for Sick Children Animal Care Committee (Toronto, ON). Male mice aged 6–10 weeks were used for experiments. Mice were maintained on a 12-hr light–dark cycle with food and water available ad libitum.

4.4 | Mouse infections and tissue preparation

Mice were infected with 2 × 10^5 cfu wild-type *Lm* in 200 µl PBS via intravenous injection in the lateral tail vein. Mice were euthanized by cervical dislocation 72-hr post-infection. Liver sections were embedded in OCT compound (Tissue-Tek, Sakura) and snap frozen in liquid nitrogen. A total of 5-µm transverse sections were taken on a cryostat (Leica CM1850) and mounted onto Superfrost Plus slides (VWR; 48311–703). Serial sections were collected and H&E stained prior to immunofluorescence imaging to ensure images were taken at the foci center rather than the periphery.

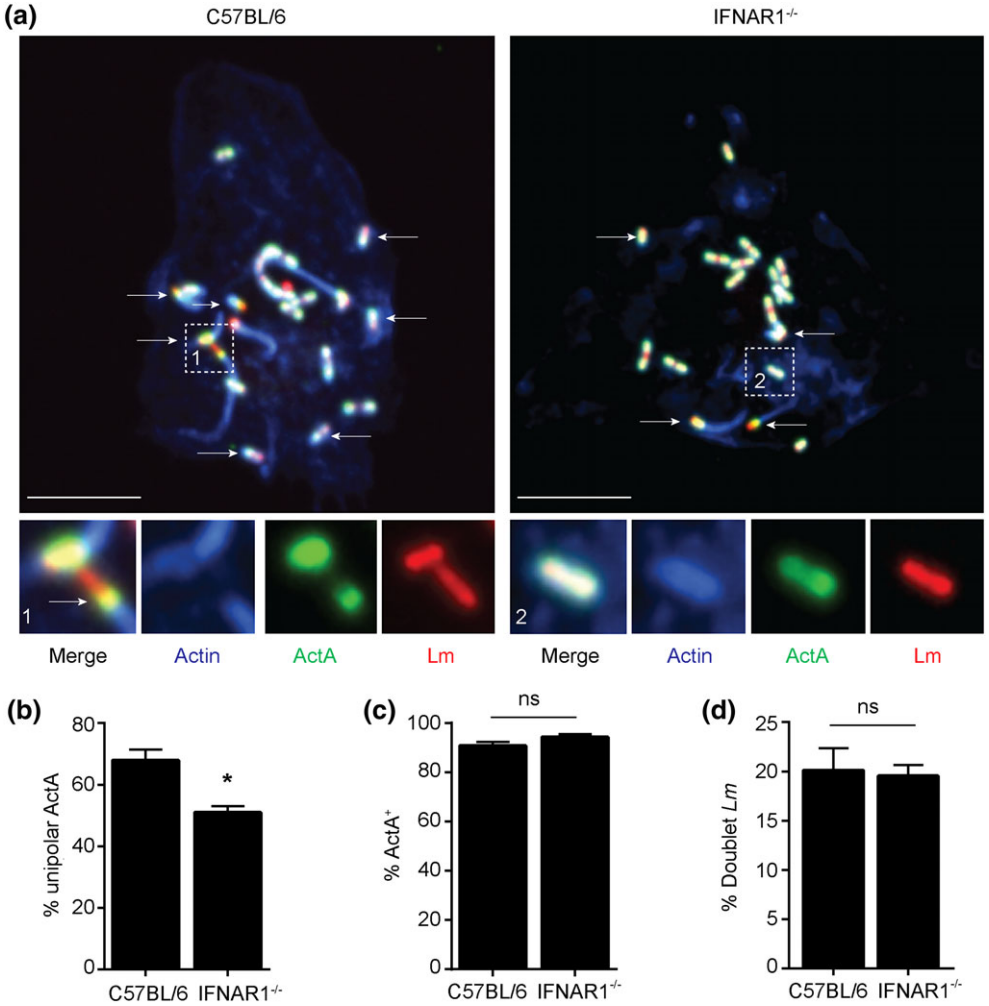

FIGURE 7 IFNAR1 promotes ActA polarization. C57BL/6 and IFNAR1$^{-/-}$ bone marrow-derived macrophages (BMDMs) were infected with RFP-*Lm* for 4 hr, stained for F-actin and ActA, and examined by confocal microscopy. (a) Representative images. Zoomed in panels highlight ActA localization along *Lm*. Arrows indicate *Lm* with polarized ActA. Scale = 11 μm. Images were used to quantify (b) the percentage of *Lm* with unipolar ActA distribution, (c) the percentage of ActA positive *Lm*, and (d) the percentage of doublet *Lm* (bacteria that had replicated but not completed septation) (n = 3, N = 20 cells, *; $p < 0.05$)

4.5 | Macrophage generation

Bone marrow-derived macrophages were generated from dissected femurs and tibias as described previously (Czuczman et al., 2014). L929 was replaced with 10% M-CSF sourced from the culture supernatant of engineered NIH-3 T3 cells (Leber et al., 2008).

4.6 | *In vitro* infection

Unless otherwise indicated, BMDMs were seeded on coverslips at 6×10^5 cells/ml 16 hr prior to infection. Using exponentially growing *Lm*, cells were infected at an MOI of 0.002 in RPMI-1640 with 10% FBS. After a 1-hr invasion, cells were washed three times with PBS (Wisent 311–420) and fresh media containing 50 μg/ml gentamicin (Wisent 311–420-CL) was added. Cells were fixed for 20 min at 37°C in 2.5% paraformaldehyde (Electron Microscopy Sciences 15710).

4.7 | Infection focus assay

Bone marrow-derived macrophages were treated with recombinant IFNβ, neutralizing anti-IFNβ or isotype control antibodies 1-hr post-infection where indicated. At 18-hr post-infection, cells were fixed and stained with rabbit anti-*Lm*, goat anti-rabbit 488, and DAPI. Infection foci were imaged using a spinning disk confocal microscope using a 10× objective. Volocity 6 software (PerkinElmer) was used to calculate the number of infected cells and area within an infection focus. At least 50 foci were imaged per condition, per biological replicate (n = 3).

4.8 | Immunofluorescence

Immunostaining of fixed cells was performed as previously described (Brumell, Rosenberger, Gotto, Marcus, & Finlay, 2001). Cells were DAPI stained 5 min then washed three times with ddH_2O. For tissue staining, sections were fixed in cold methanol (−20°C, 5 min) and permeabilized in 5% BSA (Bioship; ALB003), 15% goat serum, and 0.1% Triton-X (Bioshop; TRX506) in PBS$^{-/-}$ (Wisent; 311–010-CL). Primary antibody was diluted 1:100 into diluent (Dako S0809, 15% goat serum, 0.1% Triton-X) and placed in a hydration chamber for 24 hr at 4°C. Slides were washed three times in PBS$^{-/-}$ and secondary antibody was added for 1 hr at room temperature. Cells washed two

times in $PBS^{-/-}$ and stained with 2-μM Hoechst 33342 solution (ThermoFisher, 62249). Coverslips were mounted in fluorescence mounting medium (Dako S3023). Images were acquired using a Quorum spinning disk microscope (Leica DMI6000B inverted fluorescence microscope, Hamamatsu ORCA Flash 4 sCMOS and colour camera, spinning disk head). Images were analyzed on Volocity software. Contrast enhancement was applied evenly across images to improve clarity for publication. Images were imported and assembled in Adobe Illustrator for labeling.

4.9 | Live cell imaging

Bone marrow-derived macrophages were seeded onto six-well plate coverslips at 2×10^6 cells/ml and infected with RFP-*Lm* at an MOI of 0.002. At 6-hr post-infection, coverslips were transferred to live imaging chambers where cells were maintained at 37°C in and 25-mM HEPES (BioShop HEP001) buffered RPMI-1640, 10% FBS. Images were acquired every 15 min for 15 hr using a 10× objective on a Quorum spinning disk microscope (DMI6000B inverted fluorescence microscope, Hamamatsu ImagEMx2 camera, spinning disk head). For each biological replicate (n = 3), 10 infection foci were imaged with 0.5-μm slices (15-μm total stacks). Volocity software was used to calculate the voxel volume for each fluorescent probe. For live cell analysis of *Lm* actin-based motility, 1×10^5 cells/ml were seeded onto six-well coverslips and infected with RFP-*Lm* at an MOI of 1 and coverslips transferred to imaging chambers 4-hr post-infection. SiR-actin probe and verapamil were added to the media and incubated for 30 min at 37°C. Images were captured every 15 s for 4 min. Cells were imaged using a 63× objective with 1-μm slices (4-μm total stacks). Volocity software was used to quantify the number of *Lm*, actin recruitment, and speed of *Lm*. At least 10 cells were imaged per biological replicate. (n = 3).

4.10 | Fixed comet tail and protrusion assay

Bone marrow-derived macrophages were seeded on coverslips at 5×10^4 cells/ml and infected at an MOI of 1. Cells were fixed 7-hr post-infection and stained for immunofluorescence imaging using rabbit anti-*Lm*, goat anti-rabbit 568, mouse anti-ezrin, goat anti-mouse 488 and Phalloidin 405 antibodies. Confocal microscopy was used to image highly infected cells using 0.2-μm slices. Twenty images were analyzed per biological replicate (n = 3). Volocity software was used to quantify the number of *Lm*, the number and length of each comet tail and protrusion in each image. Comet tails were defined as being $phalloidin^+$ and $ezrin^-$, within the boundaries of the cell, and greater than 1 μm in length. Protrusions were $phalloidin^+$ and $ezrin^+$, outside the cell boundary, and greater than 1 μm in length.

4.11 | Cell-to-cell spread assay

Cell-to-cell spread assays were performed as previously described (Czuczman et al., 2014) using BMDMs from C57BL/6 and $IFNAR1^{-/-}$ mice in each genotypic combination. Fixed cells were stained using rabbit anti-*Lm*, goat anti-rabbit 488, and Phalloidin 568. Images of highly infected primary cells in contact with secondary cells (CellTracker-labeled) were acquired using confocal microscopy using 0.2-μm slices. As a control for primary cell lysis, BMDMs were infected with Δ*actA* and visually inspected. VOLOCITY software was used to analyze the total number of protrusions formed by the primary cell, the number of protrusions associated with secondary cells, and the number of *Lm* in the secondary cells. Twenty images were analyzed per biological replicate (n = 3).

4.12 | Statistical analysis

Analyses were performed using GRAPHPAD PRISM Version 6.05. Figures display the average +/− s.e.m. and p values calculated as described in figure legends. Paired student t tests were used unless otherwise stated.

ACKNOWLEDGEMENTS

We thank Mike Woodside and Paul Paroutis for their help with confocal microscopy. We are grateful to Daniel A. Portnoy (University of California at Berkeley) for providing bacterial strains.

FUNDING INFORMATION

J. H. B. holds the Pitblado Chair in Cell Biology at the Hospital for Sick Children. This work is supported by an operating grant from the Canadian Institutes of Health Research (MOP#136973). S. E. O. was supported by a Banting Fellowship from the Canadian Institutes of Health Research, a SickKids Research Training Committee Fellowship and the William P. Wilder Fellowship. B. S. was supported by a summer studentship from the Canadian Association for Gastroenterology and Crohns & Colitis Canada. E. C. was supported by the SickKids Summer Research Program. A. S. was supported by a NSERC-CGS scholarship.

CONFLICT OF INTEREST

These authors declare that there are no conflicts of interest.

REFERENCES

Alberti-Segui, C., Goeden, K. R., & Higgins, D. E. (2007). Differential function of *Listeria monocytogenes* listeriolysin O and phospholipases C in vacuolar dissolution following cell-to-cell spread. *Cellular Microbiology*, *9*, 179–195.

Auerbuch, V., Brockstedt, D. G., Meyer-Morse, N., O'Riordan, M., & Portnoy, D. A. (2004). Mice lacking the type I interferon receptor are resistant to *Listeria monocytogenes*. *The Journal of Experimental Medicine*, *200*, 527–533.

Bishop, D. K., & Hinrichs, D. J. (1987). Adoptive transfer of immunity to *Listeria monocytogenes*. The influence of in vitro stimulation on lymphocyte subset requirements. *Journal of Immunology*, *139*, 2005–2009.

Brumell, J. H., Rosenberger, C. M., Gotto, G. T., Marcus, S. L., & Finlay, B. B. (2001). SifA permits survival and replication of *Salmonella typhimurium* in murine macrophages. *Cellular Microbiology*, *3*, 75–84.

Brundage, R. A., Smith, G. A., Camilli, A., Theriot, J. A., & Portnoy, D. A. (1993). Expression and phosphorylation of the *Listeria monocytogenes* ActA protein in mammalian cells. *Proceedings of the National Academy of Sciences of the United States of America*, *90*, 11890–11894.

Brzoza-Lewis, K. L., Hoth, J. J., & Hiltbold, E. M. (2012). Type I interferon signaling regulates the composition of inflammatory infiltrates upon infection with *Listeria monocytogenes*. *Cellular Immunology*, *273*, 41–51.

Carrero, J. A., Calderon, B., & Unanue, E. R. (2004). Type I interferon sensitizes lymphocytes to apoptosis and reduces resistance to *Listeria* infection. *The Journal of Experimental Medicine*, *200*, 535–540.

Chang, W. L., Coro, E. S., Rau, F. C., Xiao, Y., Erle, D. J., & Baumgarth, N. (2007). Influenza virus infection causes global respiratory tract B cell response modulation via innate immune signals. *Journal of Immunology*, *178*, 1457–1467.

Chong, R., Squires, R., Swiss, R., & Agaisse, H. (2011). RNAi screen reveals host cell kinases specifically involved in *Listeria monocytogenes* spread from cell to cell. *PloS One*, *6*, .e23399

Czuczman, M. A., Fattouh, R., van Rijn, J. M., Canadien, V., Osborne, S., Muise, A. M., et al. (2014). *Listeria monocytogenes* exploits efferocytosis to promote cell-to-cell spread. *Nature*, *509*, 230–234.

de Souza Santos, M., & Orth, K. (2015). Subversion of the cytoskeleton by intracellular bacteria: Lessons from *Listeria*, *Salmonella* and *Vibrio*. *Cellular Microbiology*, *17*, 164–173.

Domann, E., Wehland, J., Rohde, M., Pistor, S., Hartl, M., Goebel, W., et al. (1992). A novel bacterial virulence gene in *Listeria monocytogenes* required for host cell microfilament interaction with homology to the proline-rich region of vinculin. *The EMBO Journal*, *11*, 1981–1990.

Dorhoi, A., Yeremeev, V., Nouailles, G., Weiner, J. 3rd, Jorg, S., Heinemann, E., et al. (2014). Type I IFN signaling triggers immunopathology in tuberculosis-susceptible mice by modulating lung phagocyte dynamics. *European Journal of Immunology*, *44*, 2380–2393.

Eshleman, E. M., & Lenz, L. L. (2014). Type I interferons in bacterial infections: Taming of myeloid cells and possible implications for autoimmunity. *Frontiers in Immunology*, *5*, 431.

Fattouh, R., Kwon, H., Czuczman, M. A., Copeland, J. W., Pelletier, L., Quinlan, M. E., et al. (2015). The diaphanous-related formins promote protrusion formation and cell-to-cell spread of *Listeria monocytogenes*. *The Journal of Infectious Diseases*, *211*, 1185–1195.

Gianfelice, A., Le, P. H., Rigano, L. A., Saila, S., Dowd, G. C., McDivitt, T., et al. (2015). Host endoplasmic reticulum COPII proteins control cell-to-cell spread of the bacterial pathogen *Listeria monocytogenes*. *Cellular Microbiology*, *17*, 876–892.

Grundling, A., Gonzalez, M. D., & Higgins, D. E. (2003). Requirement of the *Listeria monocytogenes* broad-range phospholipase PC-PLC during infection of human epithelial cells. *Journal of Bacteriology*, *185*, 6295–6307.

Hansen, K., Prabakaran, T., Laustsen, A., Jorgensen, S. E., Rahbaek, S. H., Jensen, S. B., et al. (2014). *Listeria monocytogenes* induces IFNbeta expression through an IFI16-, cGAS- and STING-dependent pathway. *The EMBO Journal*, *33*, 1654–1666.

Henry, T., Brotcke, A., Weiss, D. S., Thompson, L. J., & Monack, D. M. (2007). Type I interferon signaling is required for activation of the inflammasome during Francisella infection. *The Journal of Experimental Medicine*, *204*, 987–994.

Ireton, K. (2013). Molecular mechanisms of cell–cell spread of intracellular bacterial pathogens. *Open biology*, *3*, 130079.

Ireton, K., Rigano, L. A., Polle, L., & Schubert, W. D. (2014). Molecular mechanism of protrusion formation during cell-to-cell spread of *Listeria*. *Frontiers in cellular and infection microbiology*, *4*, 21.

Kocks, C., Gouin, E., Tabouret, M., Berche, P., Ohayon, H., & Cossart, P. (1992). L. monocytogenes-induced actin assembly requires the actA gene product, a surface protein. *Cell*, *68*, 521–531.

Kuehl, C. J., Dragoi, A. M., Talman, A., & Agaisse, H. (2015). Bacterial spread from cell to cell: Beyond actin-based motility. *Trends in Microbiology*, *23*, 558–566.

Lambrechts, A., Gevaert, K., Cossart, P., Vandekerckhove, J., & Van Troys, M. (2008). *Listeria* comet tails: The actin-based motility machinery at work. *Trends in Cell Biology*, *18*, 220–227.

Leber, J. H., Crimmins, G. T., Raghavan, S., Meyer-Morse, N. P., Cox, J. S., & Portnoy, D. A. (2008). Distinct TLR- and NLR-mediated transcriptional responses to an intracellular pathogen. *PLoS Pathogens*, *4*, .e6

Leung, N., Gianfelice, A., Gray-Owen, S. D., & Ireton, K. (2013). Impact of the *Listeria monocytogenes* protein InlC on infection in mice. *Infection and Immunity*, *81*, 1334–1340.

McNab, F., Mayer-Barber, K., Sher, A., Wack, A., & O'Garra, A. (2015). Type I interferons in infectious disease. *Nature Reviews. Immunology*, *15*, 87–103.

Monack, D. M., & Theriot, J. A. (2001). Actin-based motility is sufficient for bacterial membrane protrusion formation and host cell uptake. *Cellular Microbiology*, *3*, 633–647.

Muller, U., Steinhoff, U., Reis, L. F., Hemmi, S., Pavlovic, J., Zinkernagel, R. M., & Aguet, M. (1994). Functional role of type I and type II interferons in antiviral defense. *Science*, *264*, 1918–1921.

O'Connell, R. M., Saha, S. K., Vaidya, S. A., Bruhn, K. W., Miranda, G. A., Zarnegar, B., et al. (2004). Type I interferon production enhances susceptibility to *Listeria monocytogenes* infection. *The Journal of Experimental Medicine*, *200*, 437–445.

O'Riordan, M., Yi, C. H., Gonzales, R., Lee, K. D., & Portnoy, D. A. (2002). Innate recognition of bacteria by a macrophage cytosolic surveillance pathway. *Proceedings of the National Academy of Sciences of the United States of America*, *99*, 13861–13866.

Pfeffer, L. M., Kim, J. G., Pfeffer, S. R., Carrigan, D. J., Baker, D. P., Wei, L., & Homayouni, R. (2004). Role of nuclear factor-kappaB in the antiviral action of interferon and interferon-regulated gene expression. *The Journal of Biological Chemistry*, *279*, 31304–31311.

Rafelski, S. M., & Theriot, J. A. (2005). Bacterial shape and ActA distribution affect initiation of *Listeria monocytogenes* actin-based motility. *Biophysical Journal*, *89*, 2146–2158.

Rafelski, S. M., & Theriot, J. A. (2006). Mechanism of polarization of *Listeria monocytogenes* surface protein ActA. *Molecular Microbiology*, *59*, 1262–1279.

Rayamajhi, M., Humann, J., Penheiter, K., Andreasen, K., & Lenz, L. L. (2010). Induction of IFN-alphabeta enables *Listeria monocytogenes* to suppress macrophage activation by IFN-gamma. *The Journal of Experimental Medicine*, *207*, 327–337.

Rigano, L. A., Dowd, G. C., Wang, Y., & Ireton, K. (2014). *Listeria monocytogenes* antagonizes the human GTPase Cdc42 to promote bacterial spread. *Cellular Microbiology*, *16*, 1068–1079.

Robbins, J. R., Barth, A. I., Marquis, H., de Hostos, E. L., Nelson, W. J., & Theriot, J. A. (1999). *Listeria monocytogenes* exploits normal host cell processes to spread from cell to cell. *The Journal of Cell Biology*, *146*, 1333–1350.

Rusinova, I., Forster, S., Yu, S., Kannan, A., Masse, M., Cumming, H., et al. (2013). Interferome v2.0: An updated database of annotated interferon-regulated genes. *Nucleic Acids Research*, *41*, D1040–D1046.

Schneider, W. M., Chevillotte, M. D., & Rice, C. M. (2014). Interferon-stimulated genes: A complex web of host defenses. *Annual Review of Immunology*, *32*, 513–545.

Siegrist, M. S., Aditham, A. K., Espaillat, A., Cameron, T. A., Whiteside, S. A., Cava, F., et al. (2015). Host actin polymerization tunes the cell division cycle of an intracellular pathogen. *Cell Reports*, *11*, 499–507.

Skoble, J., Portnoy, D. A., & Welch, M. D. (2000). Three regions within ActA promote Arp2/3 complex-mediated actin nucleation and *Listeria monocytogenes* motility. *The Journal of Cell Biology*, *150*, 527–538.

Smith, G. A., Marquis, H., Jones, S., Johnston, N. C., Portnoy, D. A., & Goldfine, H. (1995). The two distinct phospholipases C of *Listeria*

monocytogenes have overlapping roles in escape from a vacuole and cell-to-cell spread. *Infection and Immunity*, *63*, 4231–4237.

Talman, A. M., Chong, R., Chia, J., Svitkina, T., & Agaisse, H. (2014). Actin network disassembly powers dissemination of *Listeria monocytogenes*. *Journal of Cell Science*, *127*, 240–249.

Tilney, L. G., & Portnoy, D. A. (1989). Actin filaments and the growth, movement, and spread of the intracellular bacterial parasite, *Listeria monocytogenes*. *The Journal of Cell Biology*, *109*, 1597–1608.

Tilney, L. G., DeRosier, D. J., & Tilney, M. S. (1992). How *Listeria* exploits host cell actin to form its own cytoskeleton. I. Formation of a tail and how that tail might be involved in movement. *The Journal of Cell Biology*, *118*, 71–81.

Waite, J. C., Leiner, I., Lauer, P., Rae, C. S., Barbet, G., Zheng, H., et al. (2011). Dynamic imaging of the effector immune response to *Listeria* infection in vivo. *PLoS Pathogens*, *7*, .e1001326

Welch, M. D., Iwamatsu, A., & Mitchison, T. J. (1997). Actin polymerization is induced by Arp2/3 protein complex at the surface of *Listeria monocytogenes*. *Nature*, *385*, 265–269.

SUPPORTING INFORMATION

Additional Supporting Information may be found online in the supporting information tab for this article.

How to cite this article: Osborne SE, Sit B, Shaker A, et al. Type I interferon promotes cell-to-cell spread of *Listeria monocytogenes*, *Cell. Microbiol.* 2017;**19**:e12660. https://doi.org/10.1111/cmi.12660